AJNR

Morphology of the Inner Structure of the Hippocampal Formation in Alzheimer Disease

Michito Adachi, Shinobu Kawakatsu, Takaaki Hosoya, Koichi Otani, Tsuguo Honma, Akiko Shibata and Yukio Sugai

Morphology of the Inner Structure of the Hippocampal Formation in Alzheimer Disease

Michito Adachi, Shinobu Kawakatsu, Takaaki Hosoya, Koichi Otani, Tsuguo Honma, Akiko Shibata, and Yukio Sugai

BACKGROUND AND PURPOSE: **To our knowledge, inner structural alterations of the hippocampus have never been demonstrated because of the lack of contrast between the hippocampus proper and the superficial medullary lamina. We sought to demonstrate the anatomic details of the inner hippocampus and to elucidate its alterations in Alzheimer disease (AD) in vivo.**

METHODS: **We obtained multishot diffusion- and T2-weighted MR images in 14 healthy control subjects and 26 patients with mild or moderate AD (diagnosis based on Mini-Mental Status Examination scores). We measured the width of the subiculum, CA1 and CA3–4, and the height of CA3–4 on coronal images.**

RESULTS: **The subiculum and hippocampus proper were demonstrated as whirlpool-shaped hyperintense areas, and the superficial medullary lamina was visible as a hypointense structure along the inner margin of the hippocampus proper. Regarding the width of the subiculum and CA1, intergroup analysis revealed significant differences between the control and mild or moderate AD groups. In the width of CA3–4, we found no significant difference between the control and mild AD groups; however, differences between the control and moderate AD groups and between the mild and moderate AD groups were significant. In the height of CA3–4, we observed no significant differences between groups.**

CONCLUSION: **We clearly visualized the inner structure of the hippocampal formation by using multishot diffusion-weighted imaging. The subiculum and CA1 are the most vulnerable regions in AD, and atrophy of these structures was evident in both mild and moderate AD.**

The diagnosis of mild Alzheimer disease (AD) is becoming increasingly important in aging societies, as therapies are now available to treat mild AD (1–3). In particular, the diagnosis of mild AD and indications for drug treatment have become important areas of investigation. Many studies of MR imaging have demonstrated that volumetric atrophy of the hippocampus is a sensitive indicator of AD (4–12). However, to our knowledge, the details of inner structural alterations of the hippocampal formation (the subiculum of the periallocortex, the hippocampus proper of the archicortex, and the superficial medullary lamina of the fiber bundles) have never been demonstrated because of the lack of contrast between the hippocampus proper (CA1–4 and dentate gyrus) and the superficial medullary lamina.

Recently, multishot diffusion-weighted imaging has become available for the precise depiction of nerve fibers (13–16). The aim of the present study was to demonstrate the anatomic details of the inner structures of the hippocampal formation and to elucidate the hippocampal alterations in vivo, particularly in mild AD, by using multishot diffusion-weighted imaging.

Methods

Subjects

This prospective study was approved by the ethics committee of our university. Before the MR examinations were performed, we excluded subjects younger than 50 years or older than 80 years. We confirmed that all healthy volunteers had no history of major psychiatric illness and that no volunteers or patients had the following: any episodes of head injury, dependency on illegal drugs, current alcohol abuse, cardiovascular risk factors, diabetes mellitus, or malignancy. Informed consent was obtained from each participant. Patients whose screening MR images revealed cerebral infarction, hydrocephalus, or overt brain atrophy due to Pick disease were excluded.

We examined 14 healthy volunteers as the control group (six men, eight women; age range, 54–74 years; mean age ± SD, 65.0 years ± 6.3) and 26 patients with AD. The patients had cognitive and memory impairments, and psychiatrists diag-
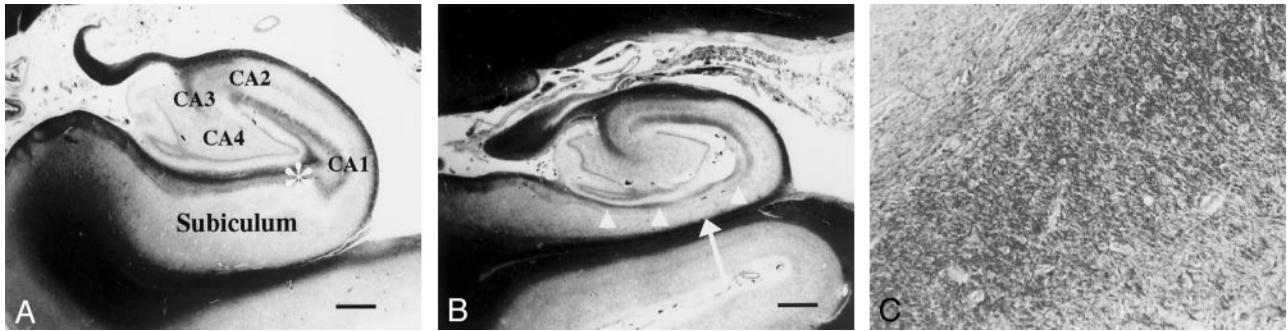
FIG 1.   Coronal photomicrographs of normal and atrophic hippocampus (Klüver-Barrera stain).

A, Image in a 56-year-old man with dentatorubro-pallidoluysian atrophy shows no atrophy of the left subiculum or hippocampus proper. Image represents a normal hippocampus. The hippocampus proper consists of the CA1, CA2, CA3, and CA4 fields. Bar indicates 1 mm.

B, Image in a 78-year-old man with AD (duration of illness, 15 years) shows severe atrophy of the subiculum (*arrow*). The superficial medullary lamina (*arrowheads*) is thinner than that of a normal hippocampus. Bar indicates 1 mm.

C, Magnified (×200) view of the image in *A* shows numerous nerve fibers running in the anteroposterior direction in the superficial medullary lamina of the hippocampal formation.

nosed their disease on the basis of the criteria established by the National Institute of Neurologic and Communicative Disorders and Stroke–Alzheimer Disease and Related Disorders Association (17). We assigned the patients with AD into mild AD and moderate AD groups. The mild AD group included 12 patients (four men, eight women; age range, 53–79 years; mean age, 67.9 years ± 7.1). Their Mini-Mental Status Examination (MMSE) scores, a practical method for grading the patient's cognitive state (18), were 25 or more at the MR imaging examination. Their mean MMSE score was 25.8 ± 0.9 and ranged from 25 to 27. In this group, the mean duration of illness was 4.2 years ± 3.4, with a range of 1–10 years. The moderate AD group included 14 patients (three men, 11 women; age range, 55–78 years; mean age, 70.0 years ± 7.8). Their MMSE scores were less than 25 at the MR imaging examination, and they had a mean MMSE score of 16.5 ± 6.2, ranging from 6 to 23. Their mean duration of illness was 4.5 years ± 2.7, with a range of 2–11 years.

MR Imaging

MR studies were performed by using a 1.5-T superconducting system (Signa; GE Medical Systems, Milwaukee, WI). For evaluating the hippocampal formation, we obtained multishot diffusion- and T2-weighted images in coronal planes that were parallel to the floor of the fourth ventricle.

Multishot diffusion-weighted images were obtained by using spin-echo echo-planar imaging with a diffusion-sensitizing gradient in the anteroposterior direction. The images showed the superficial medullary lamina as a hypointense area and the hippocampus proper as a hyperintense area, because the superficial medullary lamina along the inner margin of the hippocampus proper included a lot of nerve fibers running in the anteroposterior direction (Fig 1). The imaging parameters were as follows: TR/TE/NEX, 3000–4000/120/6; FOV, 18 × 18 cm; section thickness, 5 mm; section gap, 1 mm; matrix, 256 × 192; shots, 16; duration of the diffusion-sensitizing gradient pulses, 40 ms; diffusion-sensitizing gradient, 1.5 G/cm; gradient density factor, $b = 825$ s/mm^2; and imaging time, 5–6 minutes by using a peripheral gate. Navigator echoes were not used. The b value of 825 s/mm^2 used in this study was unusual. To obtain good contrast between the nerve fiber bundles and the surrounding brain tissues, we tried various b values ranging from 100 to 1500 s/mm^2. We found that a b value at 825 s/mm^2 provided the best contrast for visualizing the nerve fiber bundles (anterior commissure, corticospinal tract, and transverse pontine fibers).

T2-weighted images were obtained by using fast spin-echo imaging with the following parameters: TR/TE, 3540/105;
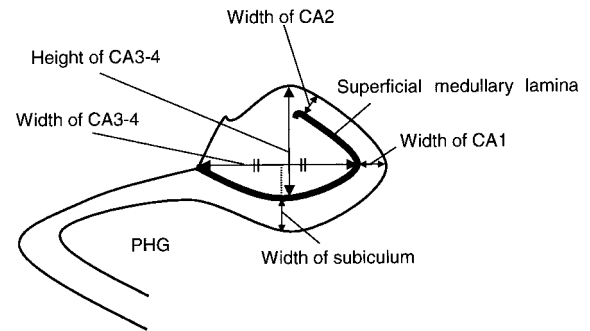

FIG 2.   Schematic representation of the hippocampal formation shows the measurement points for the subiculum and the hippocampus proper. *PHG* indicates the parahippocampal gyrus.

FOV, 18 × 18 cm; section thickness, 5 mm; section gap, 1 mm; and matrix, 256 × 256.

Measurement of the Hippocampal Formation

Two radiologists (M.A., T.H.) who had no prior knowledge of the participants' status as patients or control subjects independently measured the width of the subiculum of the periallocortex, the CA1 hippocampal field and CA3–4 field, and the height of the CA3–4 area of the hippocampal body (Fig 2). They respectively measured these areas two times by using a micrometer (minimum distance, 0.05 mm) on both multishot diffusion- and T2-weighted coronal images. These images were obtained 12 mm behind (second section from) the mammillary body and magnified to life size.

The superficial medullary lamina was visualized as a hypointense area along the inner margin of the hippocampus proper on both multishot diffusion- and T2-weighted images acquired with a diffusion-sensitizing gradient in the anteroposterior direction. The width of the subiculum was determined as the width of the hyperintense band between the superficial medullary lamina and the white matter of the parahippocampal gyrus just below the midpoint of the width of CA3–4. The width of CA1 was determined as the width of the hippocampus proper with hyperintensity at the most lateral part. We then measured the width and height of the central high-intensity of the hippocampus proper as the width and height of CA3–4.

The readers could not always measure the dimensions of the inner structure on both sides. The coincident rates of the measurability between the two readers were calculated, after which, in respective parts of the hippocampal formation, we
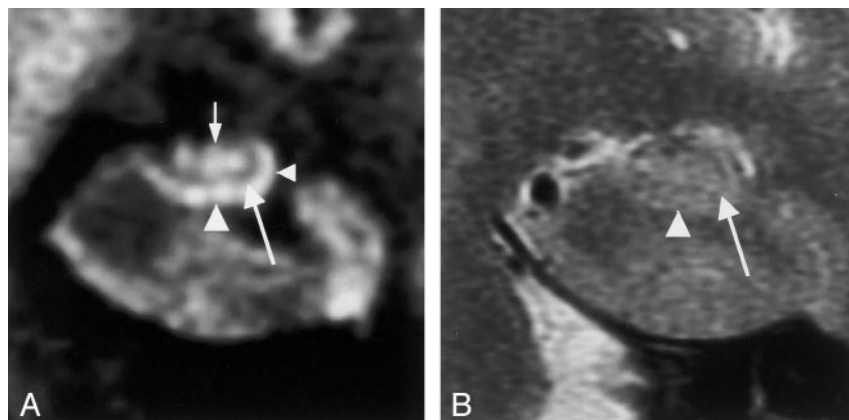
Fig 3. Coronal MR images in a 59-year-old man (control subject).

A, Multishot diffusion-weighted image clearly shows the inner structure of the left hippocampus. The subiculum (*left arrowhead*), CA1 of the hippocampus proper (*right arrowhead*), and CA3–4 (*top arrow*) are demonstrated as hyperintense areas, and the superficial medullary lamina (*bottom arrow*) is shown as a hypointense area.

B, T2-weighted image faintly shows the subiculum (*arrowhead*), the hippocampus proper, and the superficial medullary lamina (*arrow*).

excluded data for statistical analyses unless both readers were able to measure both sides.

For each site, the averaged data on both sides were calculated for the first and second measurements of the two readers. Then, we calculated the mean dimensions between the first and second measurements, after which the averaged data of the two readers were used as the final data for statistical analyses.

Statistical Analysis

Before we compared the mean dimensions, the homogeneity of variance in patients' ages was assessed by performing the Levene test. Parametric comparisons in age among groups in the measurement of various dimensions were performed by using a one-way analysis of variance (ANOVA).

To assess the intraobserver and interobserver variability error, the coefficient of variation CV% was calculated as follows: $CV\% = 100(SD_{dimension}/Mean_{dimension})$.

We also compared the dimensions of the inner hippocampal structure. For multiple group comparisons, homogeneity of variance was assessed by using the Levene test. We used one-way ANOVA to test for overall differences among groups, followed by the Tukey honestly significant difference adjustment to compare the separate group means. Statistical significance was established at the $P < .05$ level.

Results

Appearance of the Hippocampal Formation

For the visualization of the inner structure of the hippocampal formation, multishot diffusion-weighted imaging was superior to T2-weighted imaging. We found that multishot diffusion-weighted imaging offered good contrast between the hippocampus proper and the superficial medullary lamina. On multishot diffusion-weighted images, the subiculum and the hippocampus proper were demonstrated as hyperintense areas, and the superficial medullary lamina was seen as a hypointense area, resulting in a snail shell-like appearance of the hippocampal formation (Fig 3). However, the dentate gyrus could not be distinguished from CA4. CA2, the narrowest part of the hippocampus proper, was also difficult to visualize.

Measurability of Dimensions

In the measurement of the various dimensions, no significant differences were observed in the mean age among the groups, as determined with one-way

TABLE 1: Number of Cases in Which Each Part of the Hippocampal Formation Was Measurable

Measurement Site and Group	No. of Cases with Measurable Site	
	On Multishot Diffusion-Weighted Images	On T2-Weighted Images
Width of subiculum		
Control	14 (100)	1 (7)
Mild AD	10 (83)	0 (0)
Moderate AD	10 (71)	0 (0)
Width of CA1		
Control	14 (100)	3 (21)
Mild AD	11 (92)	0 (0)
Moderate AD	11 (79)	2 (14)
Width of CA3–4		
Control	14 (100)	1 (7)
Mild AD	11 (92)	1 (8)
Moderate AD	12 (86)	0 (0)
Height of CA3–4		
Control	14 (100)	2 (14)
Mild AD	10 (83)	0 (0)
Moderate AD	11 (79)	0 (0)

Note.—Data are the numbers of cases. Data in parentheses are percentages. The control group included 14 participants; the mild AD group, 12; and the moderate AD group, 14.

ANOVA. Measurability was remarkably higher with the multishot diffusion-weighted images than with the T2-weighted images. Table 1 shows the number of cases in which both readers could measure the dimensions of the bilateral hippocampal formation. According to the study design, only the data from these cases were analyzed. The dimensions of the subiculum and hippocampus proper were difficult to measure on T2-weighted images, whereas they were measurable on multishot diffusion-weighted images in all control subjects. In the patients with AD, the measurability decreased as their disease progressed. There were six patients—two with mild AD and four with moderate AD—in whom both readers could not measure at least one dimension in the bilateral hippocampal formation.

The measurability of the two readers coincided well. With the multishot diffusion-weighted images in the control group, the coincident rates of the measurability between the two readers were 100% (28 of 28) in each part. In the mild AD group, these rates were

TABLE 2: Intraobserver and Interobserver Variability

Measurement Site	Intraobserver Variability, %		Interobserver Variability %
	Observer 1	Observer 1	
Width of subiculum	9.70 ± 8.89	8.95 ± 6.09	8.34 ± 6.10
Width of CA1	6.01 ± 5.00	6.40 ± 4.27	7.97 ± 5.31
Width of CA3–4	3.91 ± 3.22	4.58 ± 4.05	4.60 ± 4.55
Height of CA3–4	6.23 ± 5.76	5.92 ± 5.56	6.99 ± 4.53

Note.—Data are the mean coefficient of variation ± standard deviation.

86% (21 of 24) for the width of the subiculum, 96% (23 of 24) for the width of CA1, 96% (23 of 24) for the width of CA3–4, and 92% (22 of 24) for the height of CA3–4. In the moderate AD group, these rates were 89% (25 of 28), 96% (27 of 28), 96% (27 of 28), and 93% (26 of 28), respectively.

Interobserver and Interobserver Variability

The coefficient of variation does not measure the correctness of measurements, only the change in the dimensions of objects in measurements of different readers. The mean intraobserver and interobserver variability for measurements is shown in Table 2. For both readers, the overall mean intraobserver variability for each measurement site was less than 10%. The mean interobserver variability was also less than 10% for each site.

Atrophy of the Inner Hippocampal Structure in AD

Visually, partial atrophy of the hippocampal formation was recognized with multishot diffusion-weighted images but not with T2-weighted images (Figs 4–7). The atrophy of the subiculum and CA1 was observed in both mild and moderate AD. With disease progression, the width of CA3–4 decreased (Figs 4–7).

The mean width of the subiculum, CA1 and CA3–4, and the height of CA3–4 on multishot diffusion-weighted images are shown in Table 3. The Levene test for assessing homogeneity of variance among the three groups revealed no significant differences in dimensions in any part of the hippocampal formation. One-way ANOVA revealed significant differences among the three groups in the dimensions of the width of the subiculum ($P < .001$), CA1 ($P < .001$), and CA3–4 ($P < .001$). However, we found no significant difference in the dimension of the height of CA3–4 ($P = .915$).

The intergroup analysis performed with the Tukey honestly significant difference adjustment indicated significant differences in the width of the subiculum between the control group and the mild AD groups ($P < .001$) or between the control group and the moderate AD group ($P < .001$). In the width of CA1, the intergroup analysis also indicated significant differences between the control group and the mild AD

groups ($P < .001$) and between the control group and the moderate AD groups ($P < .001$). In the width of CA3–4, the test showed no significant difference between the control and mild AD groups ($P = .117$); however, we observed significant differences between the control and moderate AD groups ($P < .001$) and between the mild AD and moderate AD groups ($P = .025$). In the height of CA3–4, differences between groups were not significant (Table 4).

Discussion

In this pilot study, we succeeded in determining the inner structure of the hippocampal formation in vivo by using multishot diffusion-weighted MR imaging. To our knowledge, no previous report has demonstrated alterations in the inner structure of the hippocampal formation in AD, although many groups have evaluated the volume of the hippocampal formation (4–12). Diffusion-weighted imaging was developed to measure water diffusion movement (19), and it is known to be suitable for depicting nerve fiber bundles (13–16). Photomicrographs showed that the superficial medullary lamina comprised numerous nerve fibers running in the anteroposterior direction (Fig 1). Using multishot diffusion-weighted imaging with a diffusion-sensitizing gradient in the anteroposterior direction, we succeeded in demonstrating the superficial medullary lamina as a hypointense area. Thus, the convoluted appearance of the hippocampal formation was clearly visible in all healthy control subjects, although we were unable to distinguish the dentate gyrus and CA4.

The measurability of the inner structure of the hippocampal formation was superior on multishot diffusion-weighted images compared with that on T2-weighted images. Even in patients with AD, the hippocampal formation was well depicted on multishot diffusion-weighted images. However, visualization of the superficial medullary lamina decreased somewhat in AD, especially in the moderate AD group. The pathologic findings in AD (20–23) suggest that poor visualization of the superficial medullary lamina consisting of the perforant pathway is due to severe degeneration, a characteristic feature in AD (Fig 1). Therefore, poor visualization of inner hippocampal inner structures itself might be a finding suggestive of AD. Indeed, all cases in which the inner hippocampal structures could not be measured in every part involved AD.

The measurements of the inner hippocampal structures demonstrated that atrophy of the subiculum and CA1 is a statistically significant finding in mild AD and in moderate AD; with disease progression, the width of CA3–4 decreased. Furthermore, shrinkage of the height of CA3–4 was not seen. This atrophic pattern of the hippocampal formation in patients with AD is compatible with the pathologic characteristics of the hippocampal formation in AD (20–26). The subiculum (prosubiculum) and CA1 might be the most vulnerable regions of the hippocampal formation in AD, and their atrophy might be explained by
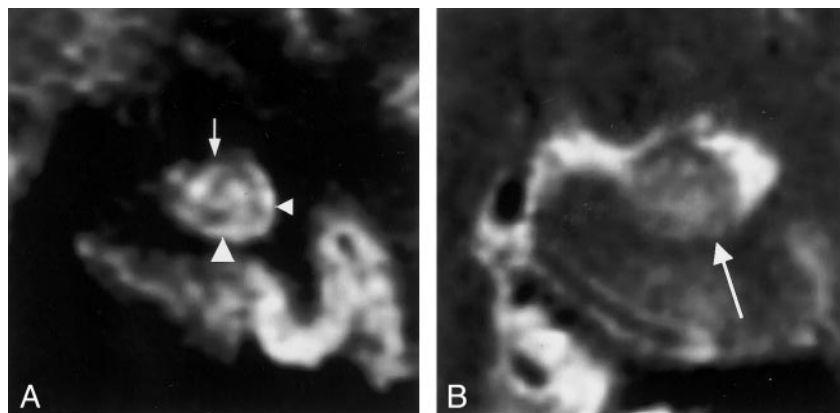
FIG 4. MR images in a 71-year-old woman with mild AD (MMSE score, 27; duration of illness, 2 years).

A, Multishot diffusion-weighted coronal image shows atrophic subiculum (*left arrowhead*) and CA1 (*right arrowhead*). However, the CA3–4 (*arrow*) is spared.

B, T2-weighted image scarcely demonstrates the inner structure of the left hippocampus (*arrow*).
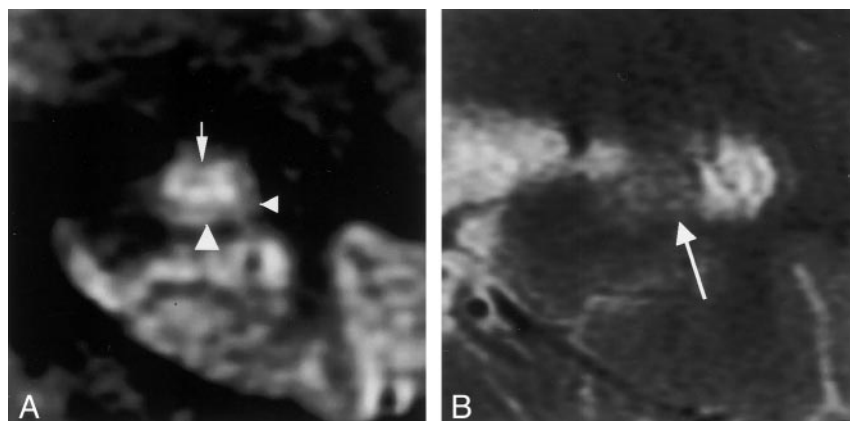

FIG 5. MR images in a 68-year-old man with mild AD (MMSE score, 25; duration of illness, 3 years).

A, Multishot diffusion-weighted coronal image shows an atrophic subiculum (*left arrowhead*) and CA1 (*right arrowhead*). CA3–4 (*arrow*) is spared.

B, T2-weighted image scarcely demonstrates the inner structure of the left hippocampus (*arrow*).

FIG 6. MR images in a 64-year-old woman with moderate AD (MMSE score, 8; duration of illness, 12 years).

A, Multishot diffusion-weighted coronal image shows an atrophic subiculum (*left arrowhead*). CA1 (*right arrowhead*) is comparatively spared; however, CA3–4 (*arrow*) is atrophic.

B, T2-weighted image scarcely demonstrates the inner structure of the left hippocampus (*arrow*).
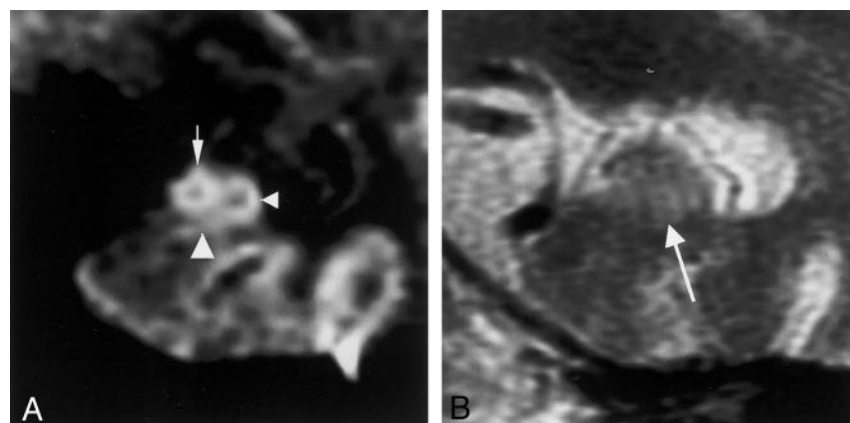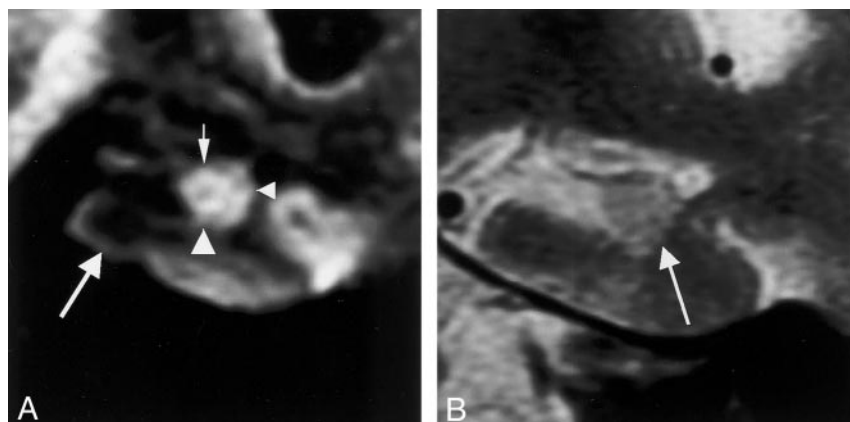

FIG 7. MR images in a 71-year-old woman with moderate AD (MMSE score, 6; duration of illness, 11 years).

A, Multishot diffusion-weighted coronal image shows severe atrophy of the subiculum (*left arrowhead*) and CA3–4 (*small arrow*). Atrophy of CA1 (*right arrowhead*) is mild. Image also shows atrophy of the parahippocampal gyrus (*large arrow*).

B, T2-weighted image barely shows the inner structure of the hippocampus (*arrow*).

TABLE 3: Mean Dimensions of Hippocampal Inner Structures in Each Group

Measurement Site	Control Group	Mild AD Group	Moderate AD Group
Width of subiculum, mm	2.60 ± 0.53	1.28 ± 0.15	1.14 ± 0.17
Width of CA1, mm	1.90 ± 0.14	1.46 ± 0.14	1.39 ± 0.19
Width of CA3–4, mm	7.18 ± 0.72	6.56 ± 0.85	5.70 ± 0.70
Height of CA3–4, mm	4.32 ± 0.57	4.30 ± 0.58	4.23 ± 0.63

Note.—Data represent the mean dimension ± standard deviation.

TABLE 4: Intergroup Analyses of the Mean Dimensions of the Inner Hippocampal Structures

Measurement Site and Comparison	DM*	SEM†	P Value	95% CI‡
Width of subiculum				
Control vs mild AD	1.32	0.15	<.001	0.95, 1.70
Control vs moderate AD	1.46	0.15	<.001	1.09, 1.83
Mild AD vs moderate AD	0.14	0.16	.688	−0.27, 0.54
Width of CA1				
Control vs mild AD	0.43	0.06	<.001	0.28, 0.59
Control vs moderate AD	0.51	0.06	<.001	0.35, 0.67
Mild AD vs moderate AD	0.08	0.07	.501	−0.09, 0.24
Width of CA3–4				
Control vs mild AD	0.62	0.30	.117	−0.12, 1.37
Control vs moderate AD	1.49	0.30	<.001	0.76, 2.21
Mild AD vs moderate AD	0.86	0.31	.025	0.09, 1.64
Height of CA3–4				
Control vs mild AD	0.02	0.24	.995	−0.58, 0.63
Control vs moderate AD	0.10	0.24	.911	−0.49, 0.68
Mild AD vs moderate AD	0.07	0.26	.955	−0.56, 0.71

Note.—Intergroup analysis was performed by using the Tukey honestly significant difference adjustment.

* Difference of the means.

† Standard error of the mean.

‡ 95% confidence interval.

the secondary change after degeneration of the superficial medullary lamina occurs. Results of pathologic studies have already suggested these hypotheses (20–23).

Coronal T1-weighted 3D volumetric spoiled gradient-recalled acquisition (SPGR) sequences have been widely used for high-resolution anatomic delineation of the hippocampal complex (9–12). However, the atrophic process of the hippocampal inner structures in AD has not been previously documented. In our experience, SPGR coronal images can demonstrate the borders between the subiculum and the white matter of the parahippocampal gyrus and between the inferior horn of the lateral ventricle and the hippocampal formation (Fig 8). However, with an SPGR sequence, which does not provide sufficient contrast
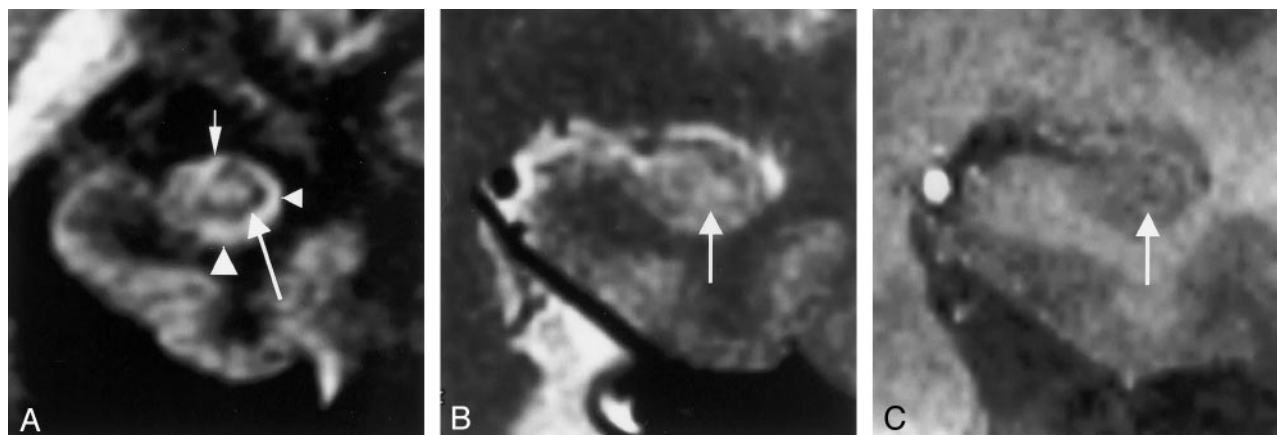

FIG 8.   MR images in a 45-year-old man (control subject).
A, Multishot diffusion-weighted coronal image clearly shows the inner structure of the left hippocampus: the subiculum (*left arrowhead*), CA1 of the hippocampus proper (*right arrowhead*), CA3–4 (*small arrow*), and the superficial medullary lamina (*large arrow*).
B, T2-weighted coronal image faintly shows the superficial medullary lamina (*arrow*) as a hypointense area.
C, T1-weighted 3D volumetric SPGR image (26/4.3; FOV, 18 cm; matrix, 256 × 256; thickness, 0.8 mm; slab, 64 mm) shows the superficial medullary lamina (*arrow*) as a hyperintense area and depicts it more faintly than does the T2-weighted image.

between the gray matter and the white matter, distinguishing the superficial medullary lamina from the subiculum and hippocampus proper in the hippocampal formation is difficult. A T2-weighted sequence might demonstrate this contrast better than an SPGR sequence (Fig 8). For this reason, we used a fast spin-echo T2-weighted sequence as a comparison for multishot diffusion-weighted imaging. Although many authors have found significant differences between control subjects and patients with mild AD when they assessed the volume of the hippocampal formation with SPGR or thin T1-weighted images (4–12), SPGR images may not be able to show partial atrophy in the hippocampal formation. In a recent article (27), investigators reported that a short–inversion time inversion-recovery (STIR) sequence offers good gray matter–white matter contrast. Although the authors used this sequence to demonstrate the substantia nigra in the midbrain of patients with Parkinson disease, this imaging method might also be useful for visualizing the inner structure of the hippocampal formation.

To our knowledge, this is the first report presenting the atrophic process of the inner hippocampal structures in AD in an in vivo study. Multishot diffusion-weighted imaging can depict partial atrophy of the hippocampal formation in AD. We also confirmed the statistical differences between control subjects and patients with mild AD. This imaging method should provide further important clues for the diagnosis of mild AD, and it is potentially useful in screening during the prodromal stage of AD.

Conclusion

We clearly visualized the inner structure of the hippocampal formation by using multishot diffusion-weighted imaging. The subiculum and CA1 are the most vulnerable regions in AD, and multishot diffusion-weighted imaging showed atrophy in these regions in mild AD.

References

1. Mohs RC, Doody RS, Morris JC, et al. **A 1-year, placebo-controlled preservation of function survival study of donepezil in AD patients.** *Neurology* 2001;57:481–488
2. Winblad B, Engedal K, Soininen H, et al. **A 1-year, randomized, placebo-controlled study of donepezil in patients with mild to moderate AD.** *Neurology* 2001;57:489–495
3. Doody RS, Geldmacher DS, Gordon B, Perdomo CA, Pratt RD. **Open-label, multicenter, phase 3 extension study of the safety and efficacy of doneprzil in patients with Alzheimer disease.** *Arch Neurol* 2001; 58:427–433
4. Lehericy S, Baulac M, Chiras J, et al. **Amygdalohippocampal MR volume measurements in the early stages of Alzheimer disease.** *AJNR Am J Neuroradiol* 1994;15:929–937
5. Dickerson BC, Goncharova I, Sullivan MP, et al. **MRI-derived entorhinal and hippocampal atrophy in incipient and very mild Alzheimer's disease.** *Neurobiol Aging* 2001;22:747–754
6. Du AT, Schuff N, Amend D, et al. **Magnetic resonance imaging of the entorhinal cortex and hippocampus in mild cognitive impairment and Alzheimer's disease.** *J Neurol Neurosurg Psychiatry* 2001; 71:441–447
7. Fox NC, Warrington EK, Freeborough PA, et al. **Presymptomatic hippocampal atrophy in Alzheimer's disease: a longitudinal MRI study.** *Brain* 1996;119:2001–2007
8. Smith CD, Malcein M, Meurer K, Schmitt FA, Markesbery WR, Pettigrew LC. **MRI temporal lobe volume measures and neuropsychologic function in Alzheimer's disease.** *J Neuroimaging* 1999;9: 2–9
9. Petersen RC, Jack CR, Xu YC, et al. **Memory and MRI-based hippocampal volumes in aging and AD.** *Neurology* 2000;54:581–587
10. Xu Y, Jack CR, O'Brien PC, et al. **Usefulness of MRI measures of entorhinal cortex versus hippocampus in AD.** *Neurology* 2000;54: 1760–1767
11. Killiany RJ, Hyman BT, Gomez-Isla T, Moss MB, Jolesz F, Jones K. **MRI measures of entorhinal cortex vs hippocampus in preclinical AD.** *Neurology* 2002;58:1188–1196
12. Hasboun D, Chantome M, Zouaoui A, et al. **MR determination of hippocampal volume: comparison of three methods.** *AJNR Am J Neuroradiol* 1996;17:1091–1098
13. Moseley ME, Cohen Y, Kcharczyk J, et al. **Diffusion-weighted MR imaging of anisotropic water diffusion in cat central nervous system.** *Radiology* 1990;176:439–445
14. Hosoya T, Adachi M, Yamaguchi K, Haku T. **MRI anatomy of white matter layers around the trigone of the lateral ventricle.** *Neuroradiology* 1998;40:477–482
15. Adachi M, Hosoya T, Haku T, et al. **Evaluation of the substantia nigra in patients with parkinsonian syndrome accomplished using multishot diffusion-weighted MR imaging.** *AJNR Am J Neuroradiol* 1999;20:1500–1506
16. Adachi M, Hosoya T, Yamaguchi K, et al. **Diffusion-weighted and T2-weighted MRI of the transverse pontine fibres in spinpcerebellar degeneration.** *Neuroradiology* 2000;42:803–809
17. McKhann G, Drachman D, Folstein M, et al. **Clinical diagnosis of Alzheimer's disease: report of the NINCDS-ADRDA Work Group under the auspices of Department of Health and Human Services Task Force on Alzheimer's disease.** *Neurology* 1984;34:939–944
18. Folstein MF, Folstein SE, McHugh PR. **Mini-mental state: a practical method for grading the cognitive state of patients for the clinician.** *J Psychiatry Res* 1975;12:189–198
19. Stejskal EO, Tenner JE. **Spin diffusion measurements: spin echoes in the presence of a time-dependent field gradient.** *J Chem Phys* 1965;42:288–292
20. Mizutani T, Kasahara M. **Degeneration of the intrahippocampal routes of the perforant and alvear pathways in senile dementia of Alzheimer type.** *Neurosci Lett* 1995;184:141–144
21. Mizutani T, Kasahara M. **Hippocampal atrophy secondary to entorhinal cortical degeneration in Alzheimer-type dementia.** *Neurosci Lett* 1997;222:119–122
22. Mizutani T, Shimada H. **Neuropathological background of twenty-seven centenarian brains.** *J Neurol Sci* 1992;108:168–177
23. Hyman BT, Van Hoesen GW, Kromer LJ, Damasio AR. **Perforant pathway changes and the memory impairment of Alzheimer's disease.** *Ann Neurol* 1986;20:472–481
24. Price JL, Ko AI, Wada MJ, et al. **Neuron number in the entorhinal cortex and CA1 in preclinical Alzheimer disease.** *Arch Neurol* 2001; 58:1395–1402
25. Bobinski M, de Leon MJ, Tarnawski M, et al. **Neuronal and volume loss in CA1 of the hippocampal formation uniquely predicts duration and severity of Alzheimer disease.** *Brain Res* 1998;805:267–269
26. Van Hoesen GW, Hyman BT. **Hippocampal formation: anatomy and the patterns of pathology in Alzheimer's disease.** *Prog Brain Res* 1990;83:445–457
27. Oikawa H, Sasaki M, Tamakawa Y, Ehara S, Tohyama K. **The substantia nigra in Parkinson disease: proton density-weighted spin-echo and fast short inversion time inversion-recovery MR findings.** *AJNR Am J Neuroradiol* 2002;23:1747–1756